Spacecraft Rendezvous and Docking with Obstacle Avoidance using Model Predictive Control

Jinaykumar Patel*
The University of Texas at Arlington, Arlington, TX 76019

Shashi Ranjan Kumar†
Indian Institute of Technology Bombay, Mumbai, India 400076

This paper addresses the problem of spacecraft rendezvous and docking to a rotating and non-rotating target spacecraft using a model predictive control approach. With this approach, the chaser is guided to the target by the relative position control, approaching in the direction of the target docking port. At the same time, the constraints on thrust, obstacle avoidance, and spacecraft positioning within the line-of-sight cone from the docking port are systematically incorporated. Numerical simulations are presented to illustrate the effectiveness and preciseness of the proposed method, along with the comparison of linear and nonlinear versions of the model predictive controller.

I. Introduction

With the increase in the space missions, rendezvous and docking (RVD) have become an integral part of almost every space mission. The autonomous RVD missions enable service and repairing of satellites and space stations, debris removal from space, refueling, etc. The RVD missions are usually concerned with the system constraints and limitations. It includes the limits on actuators (thrusters) that indeed define the control inputs. Moreover, the trajectory to the docking port on the target must be within the line-of-sight (LOS) cone to ensure the safety margin. For a tumbling target, a time varying LOS constraint must be included in the system while considering relative motion dynamics. Furthermore, the collision with the space debris must be avoided.

From the start of spaceflight history, RVD has been a crucial topic. It had been studied in great details in [1]. Control and guidance during rendezvous and docking to a stationary target in near circular orbit is the source of largest amount of research. This can be further extended for the tumbling targets in the elliptical orbits. In optimal control problems, the objective tends to be either minimizing fuel or a time or their combination. In [2], safe trajectories for autonomous rendezvous of spacecrafts while keeping the fuel consumption optimized was proposed. In the literature, different control techniques had been implemented. Glideslope, R-bar and V-bar involve an exponential decrease in velocity as the chaser spacecraft approaches the target. R-bar and V-bar are the approaches when the chaser travels along radial direction and forward velocity direction, respectively. Various tracking and control methods were performed on orbit and presented in [3], [4], [5]. Sliding mode control based method have proved to be reliable due to the guaranteed convergence after enforcement of sliding mode ([6], [7]). However, it is not optimal for either time or fuel consumption in spite of guaranteed convergence. The genetic algorithms were also utilized for the minimum fuel or time RVD problem, wherein they were useful in finding global optima in non-convex problems with multiple variables ([8], [9], [10]). However, the computational cost of genetic algorithms is large and not recommend for on-board computations. The above described methods are mainly used in ground test, that is, before the actual mission. For the missions where these techniques are used, a trajectory is already assigned to the spacecraft to follow. However, if the chaser diverges from its path then these assigned trajectories cannot be used.

The above requirements can be systematically treated using model predictive control (MPC). The MPC updates and optimizes the trajectory using the current states of the chaser and the target. Future plant outputs and control actions are predicted based on the past values. Previously, MPC had been broadly used in the process industry, followed by automotive, and now can be applicable to even more complex and critical space missions. A number of MPC strategies have been proposed to deal with RVD problem. Past research involving application of MPC in RVD focus mainly on the fixed docking port on the target. The work in [11] proposed a constraint tightening approach towards MPC. A linear quadratic MPC was implemented in [12] with the dynamic constraints for RVD. In [13], a non-linear MPC had been

*PhD Student, Department of Mechanical and Aerospace Engineering, jinaykumarnitin.patel@uta.edu, Student Member (AIAA)
†Assistant Professor, Department of Aerospace Engineering, srk@aero.iitb.ac.in, Senior Member (AIAA)

used for the trajectory optimization in RVD. A constrained MPC framework was formulated in [14], considering the LOS constraints for safe approach, soft docking constraint, and input constraints for the thruster limitations. In [14], a rotating hyper-plane method was employed to convexify the obstacle avoidance constraints.

In this paper, we account for controlling a spacecraft to approach and dock to a target using linear as well as non-linear model predictive control framework. Further, a minimum fuel optimal control problem is formulated that incorporates various constraints. Due to the physical limitation of thrusters, we have also imposed bounds on the control input. Moreover, LOS constraint and debris avoidance constraint are also imposed. Due to the simplicity of MPC and its capability to handle multiple constraints, it has been studied extensively in literature [15], [16], [17]. MPC is a powerful candidate to deal with RVD problem as it can compensate modelling uncertainties, enables superior precision with feedback control, and explicitly handles constraints present in the system, while providing guidance and control alongside the relative motion dynamic models which can be used for prediction.

The rest of the paper is organized as follows. Section II describes the problem statement and formulation where relative motion dynamics, constraints and control objective is being discussed. Section III includes the MPC controller design in detail. Further, two cases have been considered were target platform is non-rotating and rotating. Section IV includes the results obtained using MATLAB and Section V concludes the paper.

II. Problem Formulation

In this section, we formulate the problem of guiding a chaser spacecraft to dock with a target. While formulating this problem, the disturbance due to atmospheric drag, gravity gradient, solar radiation pressure, etc are neglected as these external forces are relatively much smaller than the thrust forces in the final approaching phase of RVD. It is also assumed that the target's state information can be obtained through chaser's observation and estimation. The relative motion between the chaser and the target is described through Hill-Clohessy-Wiltshere (HCW) equations ([18]). The HCW equations are restricted to the case where the target is in circular orbit and for small relative distance between target and chaser (close proximity operations). Thus, the target is assumed to be in a circular orbit with its motion confined to the orbital plane, and the target platform has a disk shape of radius r_p. In this condition, the relative dynamics described by HCW equation as follows,

$$\ddot{x} - 2n\dot{y} - 3n^2 x = \frac{F_x}{m} = u_x \tag{1}$$

$$\ddot{y} + 2n\dot{x} = \frac{F_y}{m} = u_y \tag{2}$$

$$\ddot{z} + n^2 z = \frac{F_z}{m} = u_z \tag{3}$$

where m represents the mass of the chaser, $\{F_x, F_y, F_z\}$ are the control forces of the chaser, $\{u_x, u_y, u_z\}$ are the control accelerations of the chaser, $n = \sqrt{\mu/R_T^3}$ denotes the orbital angular rate of the target, μ is the gravitational parameter for the Earth ($\mu = 3.986004418 \times 10^{14}$ m^3/s^2), and R_T is the radius of circular orbit.

The linearized continuous-time dynamical model for this problem can be formulated as

$$\dot{\mathbf{X}} = \mathbf{AX} + \mathbf{BU} \tag{4}$$

$$\mathbf{Y} = \mathbf{CX} \tag{5}$$

where $\mathbf{X}$ is the state vector, $\mathbf{U}$ is the control vector, and $\mathbf{Y}$ is the output vector. For 2-D problem, we have $\mathbf{X} = (x, y, \dot{x}, \dot{y})^T$, $\mathbf{U} = \left(u_x, u_y\right)^T$, and

$$\mathbf{A} = \begin{pmatrix} 0 & 0 & 1 & 0 \\ 0 & 0 & 0 & 1 \\ 3n^2 & 0 & 0 & 2n \\ 0 & 0 & -2n & 0 \end{pmatrix} \tag{6}$$

$$\mathbf{C} = \begin{pmatrix} 1 & 0 & 0 & 0 \\ 0 & 1 & 0 & 0 \end{pmatrix}, \quad \mathbf{B} = \begin{pmatrix} 0 & 0 \\ 0 & 0 \\ 1 & 0 \\ 0 & 1 \end{pmatrix} \tag{7}$$

Similarly, for the 3-D problem, one may have $\mathbf{X} = (x, y, z, \dot{x}, \dot{y}, \dot{z})^T$, $\mathbf{U} = \left(u_x, u_y, u_z\right)^T$, and

$$\mathbf{A} = \begin{pmatrix} 0 & 0 & 0 & 1 & 0 & 0 \\ 0 & 0 & 0 & 0 & 1 & 0 \\ 0 & 0 & 0 & 0 & 0 & 1 \\ 3n^2 & 0 & 0 & 0 & 2n & 0 \\ 0 & 0 & 0 & -2n & 0 & 0 \\ 0 & 0 & -n^2 & 0 & 0 & 0 \end{pmatrix} \tag{8}$$

$$\mathbf{C} = \begin{pmatrix} 1 & 0 & 0 & 0 & 0 & 0 \\ 0 & 1 & 0 & 0 & 0 & 0 \\ 0 & 0 & 1 & 0 & 0 & 0 \end{pmatrix}, \quad \mathbf{B} = \begin{pmatrix} 0 & 0 & 0 \\ 0 & 0 & 0 \\ 0 & 0 & 0 \\ 1 & 0 & 0 \\ 0 & 1 & 0 \\ 0 & 0 & 1 \end{pmatrix} \tag{9}$$

Note that (x, y, z) is the location of chaser and $\left(u_x, u_y, u_z\right)$ are the acceleration in three different directions in LVLH frame of reference, fixed on the target spacecraft as shown in Fig. 1. It is assumed that the acceleration is induced by the thrusters. The LVLH frame rotates with the orbit where x-direction is in the local vertical (or in radial position), y-direction is aligned with the motion of the satellite, and z-direction completes the triad.

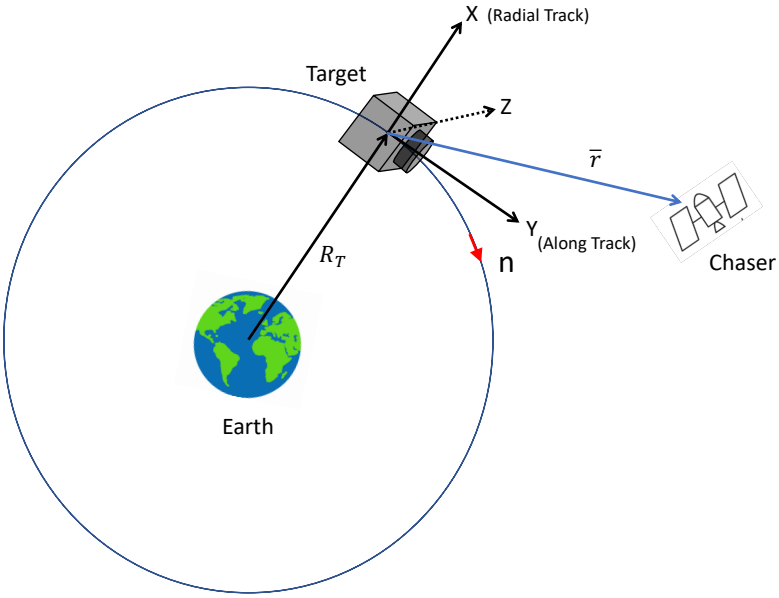

Fig. 1 The LVLH Frame of Reference.

The objective of this paper is to predict the minimum fuel proximity trajectory using the linearised HCW equations, while a receding prediction horizon control method is employed to guide the chaser to approach and dock with the target. To ensure the safe approach of the chaser, several engineering constraints such as bound on control inputs, LOS and collision avoidance constraints are implemented.

III. Model Predictive Control Design

The basic idea of the Model Predictive Control is to numerically optimize a model to obtain a sequence of control input that minimizes a cost (or objective) function over a finite control horizon, while subjected to various constraints.

The control actions are periodically re-computed at each sampling instant with the current state estimate as an initial condition, thereby providing a feedback action.

A. Prediction of States

The state-space form Eq. (4) is discretized with sampling time T_s and a discrete time model is obtained. Assuming the state and input signals at time instant k is available, we can compute the state at time $k+1$ as

$$\mathbf{X}(k+1) = \mathbf{A}_d\mathbf{X}(k) + \mathbf{B}_d\mathbf{U}(k) \tag{10}$$

where the matrices $\mathbf{A}_d$ and $\mathbf{B}_d$ are the discrete state and control matrices given by

$$\mathbf{A}_d = e^{\mathbf{A}T_s}, \quad \mathbf{B}_d = \left(\int_0^{T_s} e^{\mathbf{A}\tau} d\tau\right)\mathbf{B}$$

The predicted states generated over a finite horizon can be written as

$$\mathbf{X}_s(k+1) = \mathbf{A}_s\mathbf{X}_s(k) + \mathbf{B}_s\mathbf{U}_s(k) \tag{11}$$

where the terms $\mathbf{X}_s, \mathbf{A}_s, \mathbf{B}_s$, and $\mathbf{U}_s$ are defined as

$$\mathbf{X}_s(k) = \begin{bmatrix} x(k+1) & x(k+2) & \cdots & x\left(k+N_p\right) \end{bmatrix}^T \tag{12}$$

$$\mathbf{U}_s(k) = \begin{bmatrix} u(k) & u(k+1) & \cdots & u\left(k+N_c-1\right) \end{bmatrix}^T \tag{13}$$

$$\mathbf{A}_s = \begin{bmatrix} \mathbf{A}_d & \mathbf{A}_d^2 & \cdots & \mathbf{A}_d^{N_p} \end{bmatrix}^T \tag{14}$$

$$\mathbf{B}_s = \begin{bmatrix} \mathbf{B}_d & 0 & \cdots & 0 \\ \mathbf{A}_d\mathbf{B}_d & \mathbf{B}_d & \cdots & 0 \\ \vdots & \vdots & \ddots & \vdots \\ \mathbf{A}_d^{N_p-1}\mathbf{B}_d & \mathbf{A}_d^{N_p-2}\mathbf{B}_d & \cdots & \mathbf{B}_d \end{bmatrix} \tag{15}$$

where, N_p and N_c denote the predicted horizon and control horizon, respectively.

B. Objection Function

The primary objective of the MPC design is to minimize the tracking errors between the predicted states and the desired trajectory. Thus, the objective function, denoted as J, is defined as follows:

$$\begin{aligned} J(k) = \sum_{i=1}^{N_p} &\left\{\mathbf{X}(k+i|k) - \mathbf{X}_{\text{ref}}(k)\right\}^T \mathbf{Q} \left\{\mathbf{X}(k+i|k)\right. \\ &\left.-\mathbf{X}_{\text{ref}}(k)\right\} + \sum_{i=0}^{N_c-1} \mathbf{U}(k+i|k)^T\mathbf{R}\,\mathbf{U}(k+i|k) \end{aligned} \tag{16}$$

where $\mathbf{Q}$ and $\mathbf{R}$ are symmetric positive definite matrices which penalizes the state values and the control input, respectively. $\mathbf{X}_{\text{ref}}$ and $\mathbf{X}(k+i|k)$ are the reference trajectory and the predicted trajectory i steps ahead from the step k, respectively. $\mathbf{U}(k+i|k)$ is the control input predicted i steps ahead of k.

C. Constraints

During rendezvous and docking phase, the spacecraft must adhere to various constraints which are described as below. Depending on whether the spacecraft is in rendezvous or docking phase, different constraints are accounted for.

1. Thrust Constraint:

Each mission is constrained by a limited supply of fuel. Moreover, due to physical limits of the thrusters, the control constraints at any time instant k can be expressed as

$$u_{\min} \le u_i(k) \le u_{\max} \quad \forall \quad i = 1, 2, 3 \tag{17}$$

where $u_{\min}$ is the lower limit on thrust and $u_{\max}$ is the upper limit on thrust.

2. Line-of-Sight (LOS) Constraint:

In order to represent the safe approach corridor during the terminal phase, LOS constraints from the docking point (as shown in Fig. 2) are formulated assuming a 2-dimensional scenario. This guarantees that the chaser spacecraft is visible at all times, from the docking port of the target. The LOS constraint can be described by following equations:

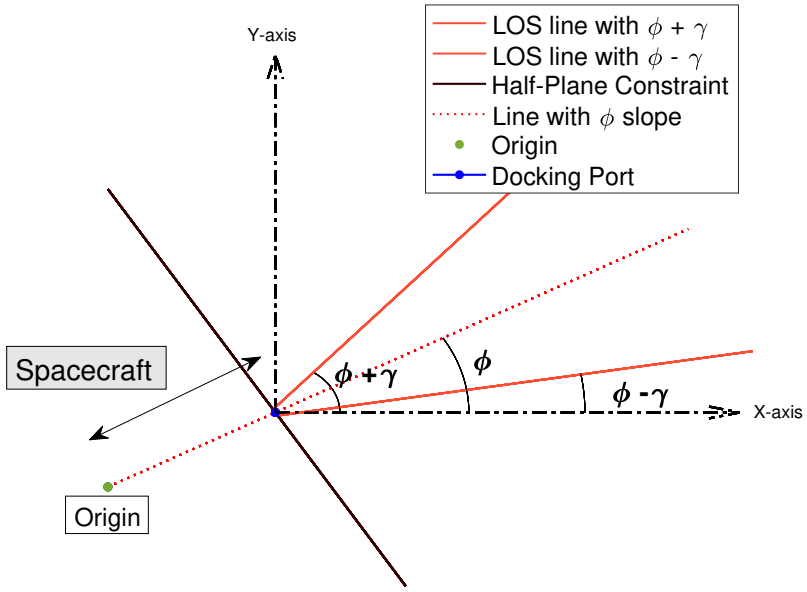

Fig. 2 Line-of-Sight Approach Cone.

$$-\frac{\sin(\varphi(k)+\gamma)}{r_p \sin\gamma}x(k) + \frac{\cos(\varphi(k)+\gamma)}{r_p \sin\gamma}y(k) \leq -1 \tag{18}$$

$$\frac{\sin(\varphi(k)-\gamma)}{r_p \sin\gamma}x(k) - \frac{\cos(\varphi(k)-\gamma)}{r_p \sin\gamma}y(k) \leq -1 \tag{19}$$

$$-\frac{\cos\varphi(k)}{r_p \sin\gamma}x(k) - \frac{\sin\varphi(k)}{r_p \sin\gamma}y(k) \leq -1 \tag{20}$$

We can rewrite the above inequality constraints as

$$\mathbf{A}_{\text{los}}\,\mathbf{X} \leq \mathbf{b}_{\text{los}} \tag{21}$$

where, the terms $\mathbf{b}_{\text{los}}$ and $\mathbf{A}_{\text{los}}$ are defined as

$$\mathbf{b}_{\text{los}} = [-1\ -1\ -1]^T$$

$$\mathbf{A}_{\text{los}} = \frac{1}{r_p \sin\gamma}\begin{bmatrix} -\sin(\varphi(k)+\gamma) & \cos(\varphi(k)+\gamma) & 0 & 0 \\ \sin(\varphi(k)-\gamma) & -\cos(\varphi(k)-\gamma) & 0 & 0 \\ -\cos\varphi(k) & -\sin\varphi(k) & 0 & 0 \end{bmatrix}$$

Here, γ is the half-cone angle, $\varphi(k)$ is the angle between the platform docking port line and the x-axis at any time instant k. Eqs. (18) and (19) correspond to the cone constraints, and Eq. (20) corresponds to the tangent line defined at the docking port (Fig. 2).

3. Obstacle Avoidance Constraint:

It must be ensured that the chaser satellite must not collide with any debris or the target, as violating this constraint can lead to worst scenarios or failure of mission. Also, the chaser should not overshoot the docking port. To implement

this constraint, the debris is assumed to be located at a point (x_d, y_d, z_d) with respect to the target frame. Further, the debris is assumed to be spherical with a radius of r_d. Mathematically, following inequality constraint must be satisfied.

$$h(x, y, z) = (x - x_d)^2 + (y - y_d)^2 + (z - z_d)^2 - r_d^2 \geq 0 \tag{22}$$

The nonlinear equation may lead to a non-convex optimization problem. Linearizing the above nonlinear equation at a point P (x_s, y_s, z_s) on the sphere tangent at line connecting centre of sphere to the chaser position (see Fig. 3).

$$\begin{aligned} &h\left(x_s + \delta x, y_s + \delta y, z_s + \delta z\right) = h\left(x_s, y_s, z_s\right) \\ &+ \left.\frac{\partial h}{\partial x}\right|_P \left(x - x_s\right) + \left.\frac{\partial h}{\partial y}\right|_P \left(y - y_s\right) + \left.\frac{\partial h}{\partial z}\right|_P \left(z - z_s\right) + \ldots \end{aligned}$$

which on neglecting higher order terms result in

$$\begin{aligned} &h\left(x_s + \delta x, y_s + \delta y, z_s + \delta z\right) \simeq h\left(x_s, y_s, z_s\right) \\ &+ 2\left(x_s - x_d\right)\left(x - x_s\right) + 2\left(y_s - y_d\right)\left(y - y_s\right) \\ &+ 2\left(z_s - z_d\right)\left(z - z_s\right) \end{aligned} \tag{23}$$

These equations are called hyperplane equations which are derived from the nonlinear sphere equations, and have been studied in literature [14]. The above equations form a boundary around the debris at each time instant. This linearization is performed at each iteration, that is, the hyperplane is rotated at a constant rate throughout the horizon. Hence, this constraints the spacecraft to remain on one side of the hyperplane. The hyperplane method provides guaranteed feasible solution due to its convex nature. This constraint is activated along the obstacle and deactivated ones the spacecraft passes the obstacle. This method can further be extended to multiple obstacles. Considering a 2-D scenario, we can rewrite Eq. (23) as,

$$\mathbf{A}_{\text{obs}}\,\mathbf{X} \leq \mathbf{b}_{\text{obs}} \tag{24}$$

where the term $\mathbf{A}_{\text{obs}}$ and $\mathbf{b}_{\text{obs}}$ are defined as

$$\begin{aligned} \mathbf{A}_{\text{obs}} &= \left[-2\left(x_s - x_d\right) \quad -2\left(y_s - y_d\right) \quad 0 \quad 0\right]^T \\ \mathbf{b}_{\text{obs}} &= h(x_s, y_s) - 2\left(x_s - x_d\right) x_o - 2\left(y_s - y_d\right) y_o \end{aligned}$$

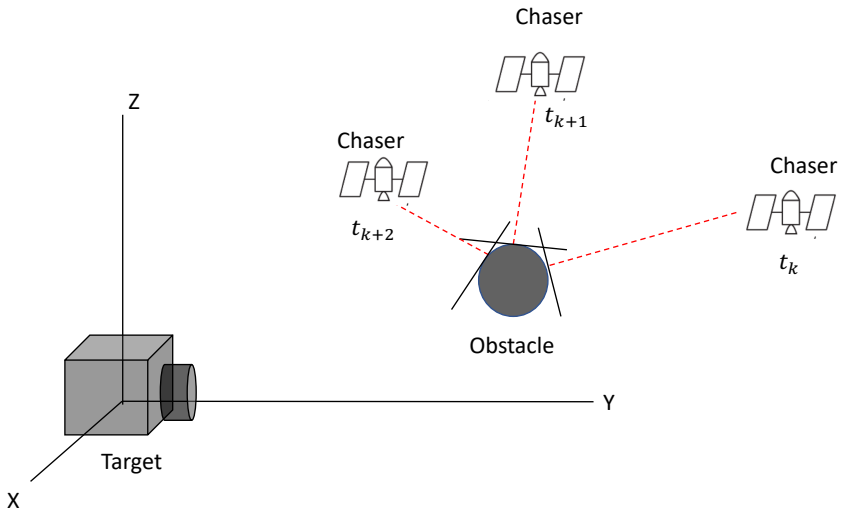

Fig. 3 Treating the debris avoidance by using hyperplanes.

Hence, the optimal control problem with the aforementioned constraints over the prediction horizon for both linear

MPC and nonlinear MPC can be formulated as follows. At every time instant k, the MPC minimises the cost function

$$\min_{\mathrm{U}(k)} \sum_{i=1}^{N_p} \left(\mathbf{X}(k+i|k) - \mathbf{X}_{\mathrm{ref}}(k)\right)^T Q \left(\mathbf{X}(k+i|k) - \mathbf{X}_{\mathrm{ref}}(k)\right) + \sum_{i=0}^{N_c-1} \mathbf{U}(k+i|k)^T R \mathbf{U}(k+i|k) \tag{25}$$

subject to the constraints given by

$$\mathbf{X}(k+1|k) = \mathbf{A}_d \mathbf{X}(k+i|k) + \mathbf{B}_d \mathbf{U}(k+i|k) \tag{26}$$

$$\left|u_j(k+i|k)\right| \leq u_{\max} \quad \forall \quad j = 1,2 \tag{27}$$

$$\left|u_j(k+i|k)\right| \geq u_{\min} \quad \forall \quad j = 1,2 \tag{28}$$

$$\mathbf{A}_{\mathrm{los}} \mathbf{X} \leq \mathbf{b}_{\mathrm{los}} \tag{29}$$

$$\mathbf{A}_{\mathrm{obs}} \mathbf{X} \leq \mathbf{b}_{\mathrm{obs}} \tag{30}$$

In order to solve this optimal control problem, the standard quadratic programming (QP) algorithm is applied using MATLAB/Simulink. The QP problem is solved at each sampling instant k to obtain a sequence of control input over a control horizon and only the first control input is implemented, then the plant state is sampled again starting from the new current state, yielding a new control and new predicted state path. For nonlinear MPC, this problem is solved using the $fmincon$ function with the Sequencial QP algorithm using MATLAB. Nonlinear MPC uses nonlinear system models for prediction.

IV. Simulations

In this section, numerical simulations of different RVD scenarios are presented to analyse the working of the proposed MPC strategy. Simulations are carried out for different initial positions of the chaser using MATLAB's MPC Toolbox on laptop computer with 8 GB RAM and 2.3 GHz Dual-Core Intel i5 processor. Both linear MPC and nonlinear MPC techniques are implemented. The LOS cone half-angle is assumed to be equal to 40° and the bounds on control input $u_{\min} = -1$ and $u_{\max} = 1$. Further, it has been considered that the target spacecraft is flying in a circular orbit at an altitude of 500 km, which means that $R_T = 6878$ km and $n = 0.0011068$ rad/s. In all simulations, the prediction horizon N_p is set as $N_p = 30$, the control horizon N_c is set as $N_c = 20$.

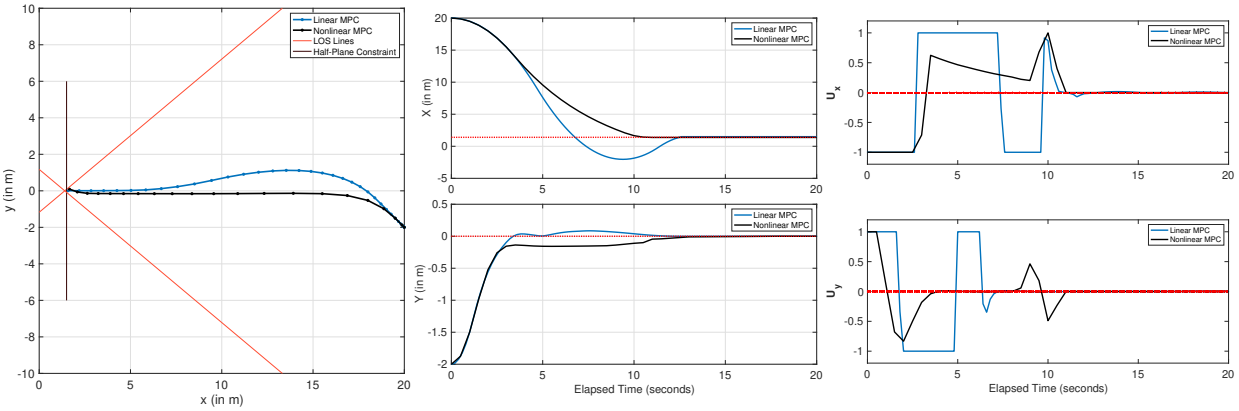

(a) Chaser trajectory **(b) Time response of the relative position** **(c) Control input**

Fig. 4 Linear and Nonlinear MPC (non-rotating target) with initial chaser position (20,-2).

A. Non-Rotating Target

In this case, the target is assumed to non-rotating with respect to its axis. As the target platform is fixed, the docking ports will also remain fixed at $(r_p \cos\phi, r_p \sin\phi)$. In this case study, the docking point is $(r_p, 0)$ with the assumption of

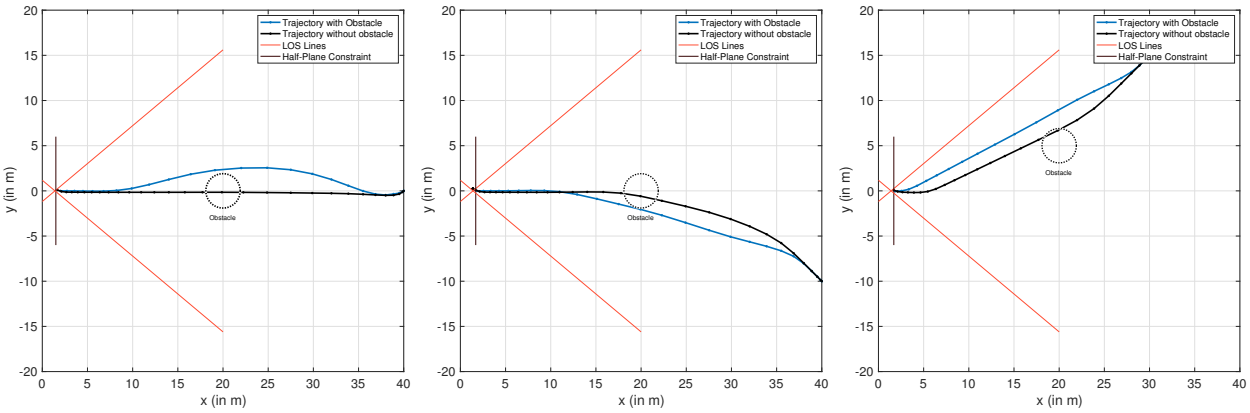

(a) Initial chaser position (40,0) **(b) Initial chaser position (40,-10)** **(c) Initial chaser position (30,15)**

Fig. 5 Nonlinear MPC for different chaser initial position with and without obstacle.

$\phi = 0$. Both linear and nonlinear MPC simulations are carried out for this case, assuming sampling time is 0.2 sec. In order to compare linear and nonlinear MPC, simulations with the same initial relative position $(20, -2)^T$ m are carried out and results are plotted in Fig. 4. It can be seen that nonlinear MPC performs the same maneuver at minimum cost but at an expense of more computational time as compared to the linear MPC. Further, it is apparent from the chaser trajecotry in Fig. 4a that the spacecraft approaches the target within LOS cone and successfully completes the maneuver. Fig. 4b indicates the time response of the relative position of chaser. The time response of control input signals is demonstrated in Fig. 4c for both linear and nonlinear MPC. It can be clearly seen that control inputs alway remain within the defined boundary, $|u| \leq 1$. Moreover, simulations are also carried out for different initial positions of chaser and obstacle to validate the optimization algorithm. The sampling time is taken as 0.5 sec. The simulated results are shown in Fig. 5, which depicts the trajectories of chaser for different initial positions of chaser $(40, 0)^T$, $(40, -10)^T$, and $(30, 15)^T$ m. For each initial position of chaser, the results are generated with and without obstacle avoidance constraints to compare the trajectories. It can be clearly seen that the obstacle avoidance technique presented in Section III can be used to avoid obstacles.

B. Rotating Target

In the previous simulations, the target spacecraft has a fixed attitude in the LVLH frame defined in Fig. 1. However, it might be possible to find situations in which the target spacecrafts is not fixed to this frame. Next, to simulate for such cases, only linear MPC is considered. The initial relative positions are assumed to be $(30, -20)^T$ m and $(-20, 40)^T$ m. For the rotating platform, the docking port $(r_p \cos\phi, r_p \sin\phi)$ will be rotating at a constant angular rate, which is evident from the time response of position in Figs. 6a and 7a as the reference trajectory is sinusoidal. It can be clearly seen that the spacecraft is successfully able to track the rotating target reference trajectory. The time response of control input signal is demonstrated in Figs. 6b and 7b for rotating target platform case. It can be clearly seen that control inputs alway remain within the defined boundary, $|u| \leq 1$.

V. Conclusion

In this paper, we proposed MPC based approach that solves the problem of spacecraft rendezvous and docking using HCW equations while satisfying the constraints. We also imposed LOS constraint for the chaser spacecraft to remain within the approach cone and the condition on control input for the chaser spacecraft due to the physical limitation on thrusters. The linear constrained equations are formed for the debris avoidance by the rotating hyper-plane method to ensure the convexity of optimization. Both linear as well as nonlinear MPC control strategies are implemented for different initial conditions. It was shown that nonlinear MPC is able to drive the chaser to track the motion of the docking port of the target while minimizing fuel consumption and satisfying all the aforementioned constraints at the expense of more extensive computational time.

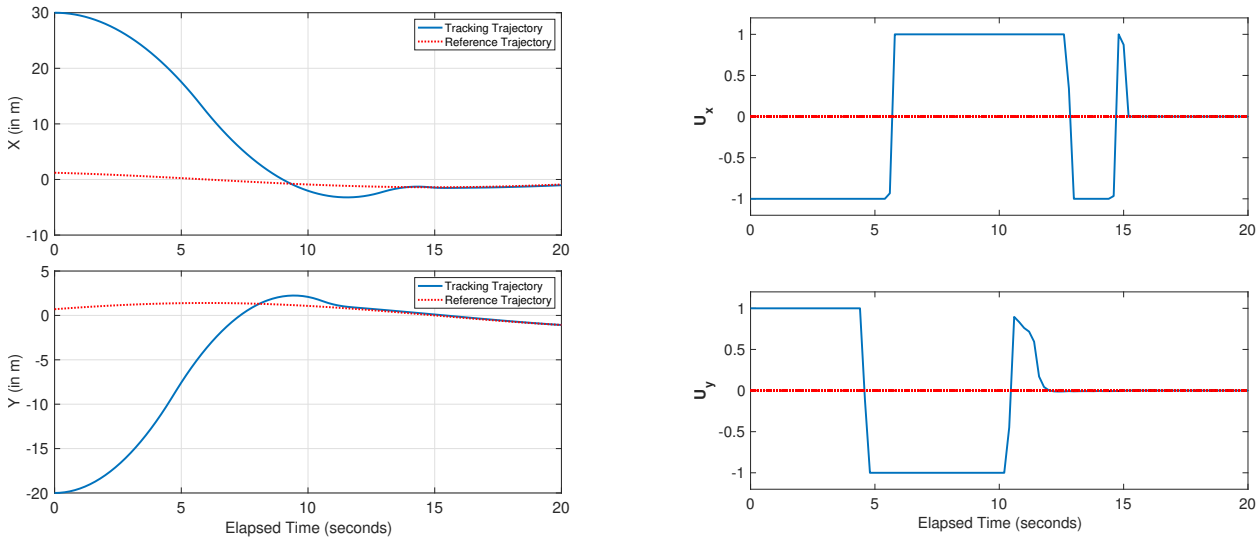

(a) Time response **(b) Control input**

Fig. 6 Rotating target with initial chaser position (30, -20).

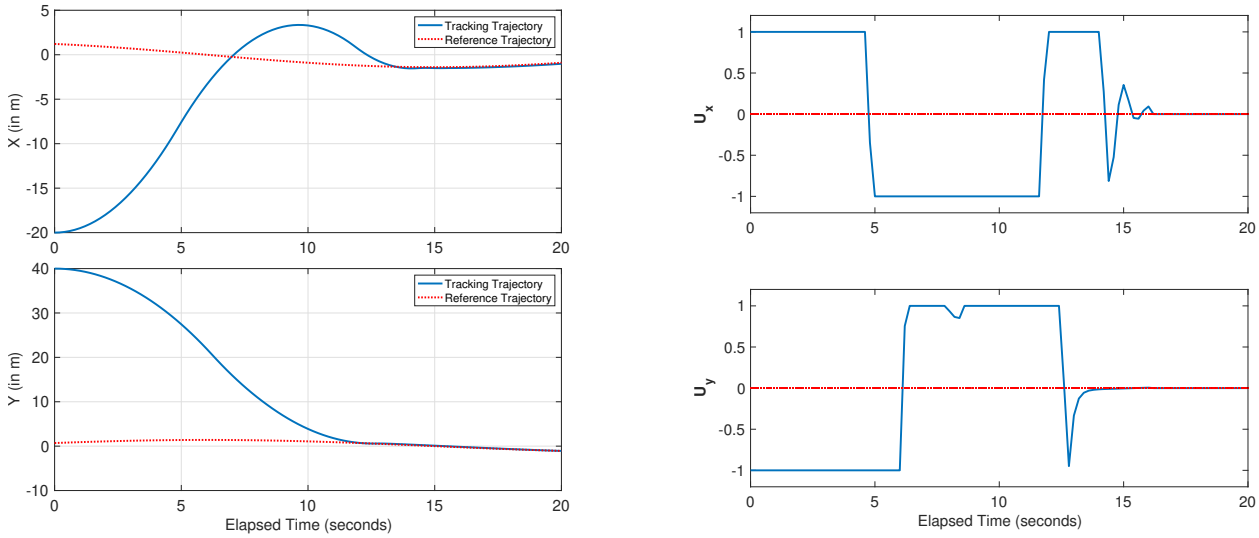

(a) Time response **(b) Control input**

Fig. 7 Rotating target with initial chaser position (-20, 40).

References

[1] Fehse, W., *Automated Rendezvous and Docking of Spacecraft*, Cambridge University Press, 2003.

[2] Breger, L., and How, J., "Safe Trajectories for Autonomous Rendezvous of Spacecraft," *Journal of Guidance Control and Dynamics*, Vol. 31, 2008. https://doi.org/10.2514/1.29590.

[3] Dana-Bashian, D., Hablani, H., and Tapper, M., "Guidance algorithms for autonomous rendezvous of spacecraft with a target vehicle in circular orbit," *AIAA Guidance, Navigation, and Control Conference and Exhibit*, 2001, p. 4393. https://doi.org/10.2514/6.2001-4393.

[4] Zanetti, R., "Optimal Glideslope Guidance for Spacecraft Rendezvous," *Journal of Guidance, Control, and Dynamics*, Vol. 34, No. 5, 2011, pp. 1593–1597. https://doi.org/10.2514/1.54103.

[5] Ariba, Y., Arzelier, D., Urbina, L. S., and Louembet, C., "V-bar and R-bar Glideslope Guidance Algorithms for Fixed-Time Rendezvous: A Linear Programming Approach," *IFAC-PapersOnLine*, Vol. 49, No. 17, 2016, pp. 385–390. https://doi.org/10.1016/j.ifacol.2016.09.066.

[6] Yang, J., and Stoll, E., "Adaptive Sliding Mode Control for Spacecraft Proximity Operations Based on Dual Quaternions," *Journal of Guidance, Control, and Dynamics*, Vol. 42, No. 11, 2019, pp. 2356–2368. https://doi.org/10.2514/1.G004435.

[7] Tournes, C., and Shtessel, Y., "Automatic Docking Using Optimal Control and Second Order Sliding Mode Control," *AIAA Guidance, Navigation and Control Conference and Exhibit*, 2007. https://doi.org/10.2514/6.2007-6345.

[8] Luo, Y.-Z., Li, H.-Y., and Tang, G.-J., "Hybrid Approach to Optimize a Rendezvous Phasing Strategy," *Journal of Guidance, Control, and Dynamics*, Vol. 30, No. 1, 2007, pp. 185–191. https://doi.org/10.2514/1.20232.

[9] Li, S., Mehra, R., Smith, R., and Beard, R., "Multi-spacecraft trajectory optimization and control using genetic algorithm techniques," *2000 IEEE Aerospace Conference. Proceedings*, Vol. 7, 2000, pp. 99–108. https://doi.org/10.1109/AERO.2000.879279.

[10] Kim, Y. H., and Spencer, D. B., "Optimal Spacecraft Rendezvous Using Genetic Algorithms," *Journal of Spacecraft and Rockets*, Vol. 39, No. 6, 2002, pp. 859–865. https://doi.org/10.2514/2.3908.

[11] Iskender, O., Ling, K., and Dubanchet, V., "Constraints Tightening Approach Towards Model Predictive Control Based Rendezvous and Docking with Uncooperative Targets," *2018 European Control Conference (ECC)*, 2018, pp. 380–385. https://doi.org/10.23919/ECC.2018.8550224.

[12] Weiss, A., Baldwin, M., Erwin, R. S., and Kolmanovsky, I., "Model Predictive Control for Spacecraft Rendezvous and Docking: Strategies for Handling Constraints and Case Studies," *IEEE Transactions on Control Systems Technology*, Vol. 23, No. 4, 2015, pp. 1638–1647. https://doi.org/10.1109/TCST.2014.2379639.

[13] Ravikumar, L., Padhi, R., and Philip, N. K., "Trajectory optimization for Rendezvous and Docking using Nonlinear Model Predictive Control," *IFAC-PapersOnLine*, Vol. 53, No. 1, 2020, pp. 518–523. https://doi.org/10.1016/j.ifacol.2020.06.087.

[14] Park, H., Zagaris, C., Virgili Llop, J., Zappulla, R., Kolmanovsky, I., and Romano, M., "Analysis and Experimentation of Model Predictive Control for Spacecraft Rendezvous and Proximity Operations with Multiple Obstacle Avoidance," *AIAA/AAS Astrodynamics Specialist Conference*, 2016. https://doi.org/10.2514/6.2016-5273.

[15] Hartley, E. N., Trodden, P. A., Richards, A. G., and Maciejowski, J. M., "Model predictive control system design and implementation for spacecraft rendezvous," *Control Engineering Practice*, Vol. 20, No. 7, 2012, pp. 695–713. https://doi.org/10.1016/j.conengprac.2012.03.009.

[16] Pascucci, C. A., Bennani, S., and Bemporad, A., "Model predictive control for powered descent guidance and control," *2015 European Control Conference (ECC)*, 2015, pp. 1388–1393. https://doi.org/10.1109/ECC.2015.7330732.

[17] Burak, I. O., "Model predictive control for spacecraft rendezvous and docking with uncooperative targets," Ph.D. thesis, Nanyang Technological University, 2020. https://doi.org/10.32657/10356/144018.

[18] Hablani, H. B., "Autonomous Inertial Relative Navigation with Sight-Line-Stabilized Sensors for Spacecraft Rendezvous," *Journal of Guidance, Control, and Dynamics*, 2012. https://doi.org/10.2514/1.36559.